Fish and Shellfish Immunology 88 (2019) 1–8

Contents lists available at ScienceDirect

Fish and Shellfish Immunology

journal homepage: www.elsevier.com/locate/fsi

Full length article

Interaction of the small GTP-binding protein (Rab7) with β-actin in *Litopenaeus vannamei* and its role in white spot syndrome virus infection

Jixing Feng*, Denglai Li, Liming Liu, Yongzheng Tang, Rongbin Du

Laboratory of Pathology of Aquatic Animals, Yantai University, Yantai, 264005, PR China

ARTICLE INFO

Keywords:
Rab7
β-Actin
White spot syndrome virus
Litopenaeus vannamei

ABSTRACT

In this study, GST Pull-down and mass spectrometry was applied to the precipitation and identification of the small GTP-binding protein (Rab7) interacting protein in hemocyte of *Litopenaeus vannamei*. According to the search in GenBank with the peptide mass fingerprint, the 45 kDa protein which was pulled down with the GST-tagged Rab7 (GST-Rab7, GTP bound form) was identified to be β-actin with 28% coverage of amino acid sequences. The interaction of Rab7 with β-actin was verified by both GST Pull-down and ELISA *in vitro*. Meanwhile, confocal microscopic observation showed that Rab7 could be co-localized with β-actin in hemocytes at 12 h post white spot syndrome virus (WSSV) infection (hpi). GST Pull-down and western blotting were used to analyze the cross-interaction between WSSV VP28, Rab7 and β-actin. The results showed that the GST-VP28, His-tagged Rab7 (His-Rab7) and His-β-actin formed a tripartite complex. At 12 hpi, confocal microscopic observation showed that WSSV could be co-localized with Rab7 and β-actin in hemocytes respectively. Furthermore, based on the *in vivo* neutralization assay, recombinant His-β-actin accelerated the infection of WSSV, conversely, recombinant His-Rab7 delayed WSSV infection in shrimp. These results suggested the interaction of Rab7 with β-actin and this interaction was involved in WSSV infection.

1. Introduction

As a key regulator in endo-lysosomal trafficking, the small GTP-binding protein Rab7 has been investigated extensively to govern early-to-late endosomal maturation, microtubule (MT) minus-end as well as plus-end directed endosomal migration and positioning, and endosome-lysosome transport through different protein-protein interaction cascades [1–3]. In *Penaeus monodon*, Rab7 has been confirmed specific binding to the major envelope protein of white spot syndrome virus (WSSV) VP28 and involving in WSSV infection through *in vivo* neutralization assay [4]. Rab7 gene in several shrimp, such as *P. monodon*, *Litopenaeus vannamei*, and *Marsupenaeus japonicus*, has been targeted by sequence-specific dsRNA, and shown to be effective in promoting shrimp survival, as well as in interfering with WSSV replication [5–7].

Coincidently, caveolin and clathrin-mediated endocytosis has been well documented in WSSV entry into the host cell of *L. vannamei* and *Cherax quadricarinatus* respectively [8–10]. Taken together, Rab7 might have an intimate connection with WSSV transport. However, the information on Rab7 and its effectors in shrimp was still limited. The vital role in MT minus-end directed transport of WSSV needs to be clarified for Rab7 and its downstream effectors, such as RILP (Rab7-interacting lysosomal protein), ORP1L (OSBP (oxysterol-binding protein) related protein) and HOPs [11–16].

In the present work, GST Pull-down and mass spectrometry were applied to the precipitation and identification of Rab7 interacting proteins in hemocyte of *L. vannamei*. The cross-interactions between WSSV VP28 and Rab7, β-actin were confirmed by GST Pull-down and western blotting. Immunofluorescence confocal microscopy and *in vivo* neutralization were used to investigate the role of Rab7 and its interacting proteins in WSSV infection. The resultant data would facilitate better understanding of WSSV transport in host cells.

2. Materials and methods

2.1. Shrimp

Adult shrimp (*L. vannamei*) with an average length of 15 cm were obtained from a commercial shrimp farm located in Yantai, Shandong, PR China and confirmed to be WSSV-free by two-step PCR with nested primer sets [17]. The shrimp were acclimated for 1 week in tanks filled with sea water of 30‰ salinity and provided with continuous aeration using electric air-pumping compressors. Half the tank water was changed at a time and the water was changed twice a week. The water temperature was 24 ± 1 °C.

* Corresponding author.
E-mail address: jxfeng2014@ytu.edu.cn (J. Feng).

https://doi.org/10.1016/j.fsi.2019.02.053
Received 25 January 2019; Received in revised form 21 February 2019; Accepted 25 February 2019
Available online 28 February 2019

Table 1
Names and sequences of primers used in this paper. The restriction sites are underlined.

Name	Sequence (5′–3′)
Rab7-His/GST-F	CCGAATTCATGGCATCTCGCAAGAAGAT
Rab7-His/GST-R	CTGTCGACTTAGCAAGAGCATGCATCCT
VP28-GST-F	CCGAATTCCGCACAGACAATATCGAGAC
VP28-GST-R	CTGTCGACTTACTCGGTCTCAGTGCCAG
β-actin-His-F	CCGAATTCATGTGTGACGACGAAGTAGC
β-actin-His-R	CTGTCGACTTAGAAGCACTTCCTGTGAAC

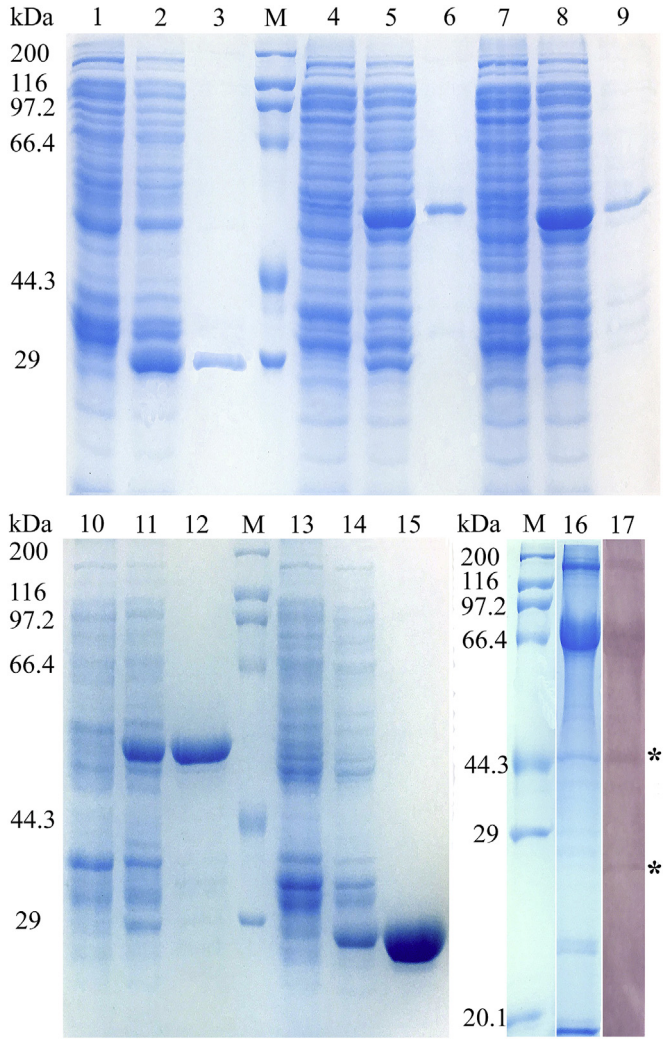

Fig. 1. SDS-PAGE and western blotting confirmed the expression of His/GST-Tagged recombinant proteins and the specificity of Abs against corresponding proteins respectively. Rab7 and β-actin in hemocyte lysate are shown as (*). Lane M, Molecular mass marker; lane 1, 4, 7, 10, 13, protein profile of uninduced BL21 cell lysate; lane 2, 5, 8, 11, 14, protein profile of induced BL21 cell lysate; lane 3, 6, 9, 12, 15, purified GST, GST-Rab7, GST-VP28, His-β-actin, His-Rab7; lane 16, protein profile of hemocyte lysate; lane 17, mouse anti-Rab7 Mab and rabbit anti-β-actin-PAbs recognized Rab7 and β-actin in hemocyte lysate respectively.

2.2. Expression of recombinant proteins

Primers β-actin-His-F and β-actin-His-R, Rab7-His/GST-F and Rab7-His/GST-R, VP28-GST-F and VP28-GST-R were used to amplify sequence of β-actin, Rab7 and VP28 which were obtained from GenBank of NCBI under accession nos. AF300705.2, FJ811529.1 and AY249434.1 respectively. The amplified products were inserted into pET-28a/pGEX-4T-1 vector and expressed as His/GST-tagged fusion protein in *Escherichia coli* BL21 (DE3). Expression and purification of the recombinant proteins were performed according to the manual of HisTrap HP (GE Healthcare Life Sciences, USA) and BeyoGold™ GST-tag Purification Resin (Beyotime Biotech, China). The expression and purification of recombinant proteins were analyzed by 12% SDS-PAGE. All the primers used in this part were listed in Table 1. The specificity of rabbit anti-β-actin polyclonal antibodies (Pabs, ZSGB-BIO, China) and mouse anti-Rab7 monoclonal antibody (Mab) (Santa Cruz, USA) against β-actin as well as Rab7 in hemocyte were identified by western blotting.

2.3. GST pull-down and identification of Rab7 interacting protein

100 μg GST-tagged Rab7 (GST-Rab7) were coupled to 30 μl glutathione beads in PBS for 2 h at 4 °C. Beads were washed and equilibrated with 0.01 M phosphate-buffered saline (PBS). Then, the beads were incubated with 100 μM GTP/GDP for 10 min at room temperature, after which $MgCl_2$ was added to a final concentration of 10 mM and the incubation was continued for an additional 30 min. GST-Rab7 was replaced with GST as control.

The hemocytes were lysed by 20 mM HEPES, 150 mM NaCl, 5 mM $MgCl_2$, 1% NP-40 pH 7.4 at 4 °C for 30 min. Cells were passed through a 26 gauge needle and centrifuged at 10, 000 × *g* for 10 min at 4 °C. The supernatant was added to the beads and incubated in a total volume of 0.5 ml for 2 h at 4 °C. Beads were washed extensively with lysis buffer, and bound proteins were separated by 12% SDS-PAGE. The suspected band was excised and subjected to matrix-assisted laser desorption/ionization MS/MS. The MS/MS result was analyzed by *m/z* software and interpreted using MASCOT (Matrix Science) against the National Center for Biotechnology Information non-redundant database.

2.4. ELISA

Flat-bottomed 96-well ELISA plates (Corning Costar, USA) were coated with 2 μg His-tagged β-actin (His-β-actin in 0.1 Mbicarbonate/carbonate buffer, pH 9.6; 100 μl per well), 10 μg hemocyte lysate solution as described in section 2.3 or 2 μg BSA (used as control) and incubated overnight at 4 °C. EDTA was added to the hemocyte lysate with a final concentration of 0.5 M to eliminate the endogenous enzyme background [18]. Plates were then washed three times with PBST (PBS containing 0.05% Tween-20), and blocking buffer (PBST with additional 1% BSA) was added, followed by incubation for 2 h at 37 °C. After washing with PBST, various dilutions (0 ng, 100 ng, 200 ng, 400 ng, 800 ng) of His-Rab7 in blocking buffer were added to plates, followed by incubation for 1 h at 37 °C.

For testing the binding of His-Rab7 to His-β-actin, plates were washed and a blocking buffer diluted mouse anti-Rab7 Mab (Santa Cruz, USA) was added (100 μl per well), followed by incubation for 1 h at 37 °C. Mouse anti-Rab7 Mab was replaced with mouse anti-6 × His Tag Mab (Sangon Biotech, China) to test the binding of His-Rab7 to hemocyte lysate.

After washing, HRP-labeled goat anti-mouse antibody (Sigma-Aldrich, USA) was added to plates, and reaction mixtures incubated for an additional 1 h at 37 °C. The reaction was visualized using the HRP substrate TMB (3,3′,5,5′-tetramethylbenzidine; Sangon Biotech). An ELISA reader (Biotech, USA) was used to read the absorbance immediately at 450 nm. Each experiment was done in triplicate. The data were given in terms of OD_{450} as means ± standard deviation (SD) (n = 3) and subjected to oone-way ANOVA followed by a multiple comparison. The *p* values less than 0.05 were considered statistically significant.

2.5. Cross-interaction between WSSV VP28, Rab7 and β-actin

To verify the interaction of Rab7 with β-actin, GST-Rab7 coupled beads (GTP bound form) were used to pull down His-β-actin (10 μg) and

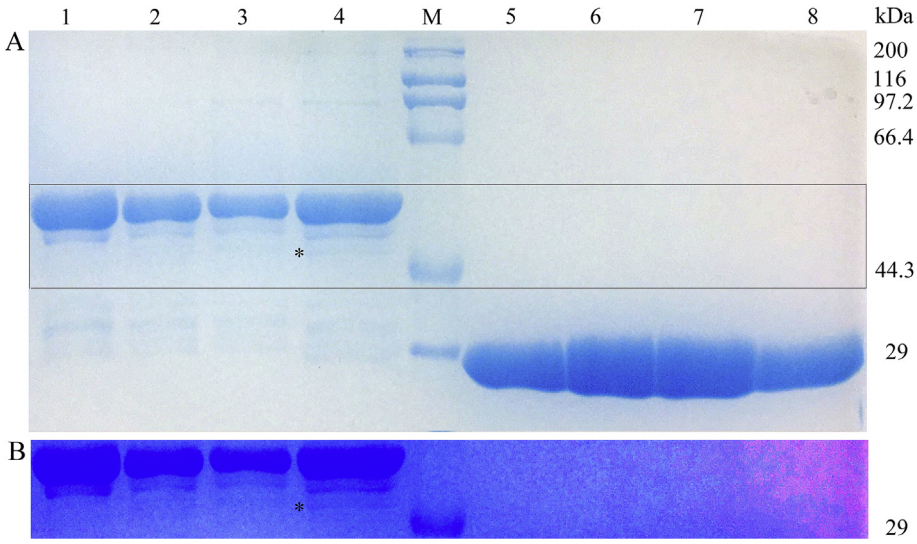

Fig. 2. Precipitation of the Rab7 interacting proteins in hemocyte by GST Pull-down. The protein precipitated with GTP-bound GST-Rab7 was marked with asterisk (*) in lane 4. A, the profiles of proteins pulled down from hemocyte lysate with GST-Rab7, GDP-bound GST-Rab7, GTP-bound GST-Rab7 were shown in lane 2, 3, 4 respectively. GST-Rab7 coupled to glutathione beads was shown in lane 1. The profiles of proteins pulled down from hemocyte lysate with GST incubated with GTP, GST incubated with GDP, GST were shown in lane 5, 6, 7 respectively. GST coupled to glutathione beads was shown in lane 8; B, the color of the bands indicated in the square frame was deepened to clearly show the protein band pulled down with GTP-bound GST-Rab7.

hemocyte lysate (20 μg), which was diluted in 500 μl GST pull-down binding buffer (Tris-HCl, 50 mM; NaCl, 200 mM; EDTA, 1 mM; NP-40, 1% (v/v); DTT, 1 mM; $MgCl_2$, 10 mM, pH 8.0) respectively.

To investigate the cross-interaction between WSSV VP28, Rab7 and β-actin, His-Rab7 (10 μg), the mixture of His-Rab7 (10 μg) and His-β-actin (10 μg), which was diluted in 500 μl GST pull-down binding buffer, was incubated with GST-VP28 coupled beads respectively. GTP was added to the GST pull-down binding buffer with the final concentration of 100 μM.

After extensive washing, the retained proteins with GST-Rab7 and GST-VP28 were analyzed by SDS-PAGE and western blotting using both rabbit anti-β-actin Pabs and mouse anti-Rab7 Mab.

2.6. Confocal microscopy

Each WSSV-free shrimp was injected with 1×10^6 virus copies diluted in 100 μl PBS through the lateral area of the third abdominal segment. Hemocytes of shrimp at 12 h post infection (hpi) were collected. The density of sampled hemocytes was adjusted to 1×10^8 cells ml^{-1}. The cell suspension was settled onto clean glass slides, after 1 h subsiding in a moist chamber, the cells were fixed in acetone for 15 min and then air-dried. After blocking in PBS containing 4% BSA, the hemocytes were incubated with antibodies at 4 °C overnight as follows: 1) rabbit anti-β-actin Pabs diluted at 1:3000 and mouse anti-WSSV Mab (obtained from Laboratory of Pathology and Immunology of Aquatic Animals, Ocean University of China) diluted at 1:500; 2) rabbit anti-β-actin Pabs and mouse anti-Rab7 Mab diluted at 1:200; 3) mouse anti-WSSV Mab and mouse anti-Rab7 Mab labeled with APEX™ Alexa Fluor™ 488/647 Antibody Labeling Kit respectively (Thermo Fisher, USA). After washing with PBST three times, fluorescein isothiocyanate (FITC)/CY3-conjugated sheep anti-mouse/rabbit IgG antibody diluted at 1:250 (Sigma-Aldrich, USA) were added onto the sample and incubated for 1 h at 37 °C. At last, the slides were wet mounted with anti-fading polyvinyl alcohol medium DABCO (Beyotime Biotech, China) and the fluorescent signals were observed with a confocal microscope fitted with a UV microscopy apparatus.

2.7. In vivo neutralization

For the challenge experiments, the protocol was performed as described previously [19]. Shrimp were divided into five groups with three replicates of 23 shrimp in each group which were applied to the recording of the cumulative mortality. Each WSSV-free shrimp was injected with a constant volume (50 μl in PBS) 1×10^6 virus copies being mixed with different amount of the recombinant proteins. Shrimp were injected as follows: group 1 with WSSV (positive control), group 2 with PBS (negative control), group 3 with WSSV plus His-Rab7 (5 μmol/shrimp), group 4 with WSSV plus His-β-actin (5 μmol/shrimp), group 5 with WSSV plus both His-Rab7 (2.5 μmol/shrimp) and His-β-actin (2.5 μmol/shrimp) as the recombinant protein test. The recombinant protein-plus WSSV preparations were mixed to the same volume (100 μl) and immediately injected into the experimental shrimp. Cumulative mortality after WSSV injection was recorded as means ± SD (n = 3).

3. Results

3.1. Expression of recombinant proteins and characterization of the specificity of Abs

His-β-actin, His/GST-Rab7 and GST-VP28 were successfully expressed in *E. coli* BL21 (DE3) with expected molecular weights (Fig. 1). High purity GST, GST-Rab7, GST-VP28 were obtained by glutathione affinity chromatography (Fig. 1, lane 3, 6, 9). High purity His-β-actin and His-Rab7 were obtained by nickel chelate affinity chromatography (Fig. 1, lane 12, 15). The Abs were identified to recognize Rab7 and β-actin (Fig. 1, lane 17) in hemocyte by western blotting.

3.2. Precipitation of Rab7 interacting proteins in hemocyte

GST pull-down experiment was used to precipitate the Rab7 interacting proteins in hemocyte. Glutathione beads effectively pulled down both GST and GST-Rab7, although the pull-down efficiency was higher with GST (Fig. 2, lanes 5–8) than with GST-Rab7 (Fig. 2, lanes 1–4). One 45 kDa protein band was only present in the pull-down product of GTP-bound GST-Rab7 (Fig. 2, lane 4). The GST controls (Fig. 2, lane 5–8), GDP-bound GST-Rab7 (Fig. 2, lane 3) and GST-Rab7 (Fig. 2, lane 2) showed no co-precipitation of hemocyte protein.

3.3. Identification of 45 kDa protein

In order to further identify the Rab7 interacting protein, the 45 kDa protein band in SDS-PAGE was excised and subjected to mass spectrometry. According to the search in GenBank with the peptide mass fingerprint (Fig. 3B), the 45 kDa protein was identified to be *L. vannamei* β-actin with 28% coverage of amino acid sequences (Fig. 3A).

A

```
  1 MCDDEVAALV VDNGSGMCKA GFAGDDAPRA VFPSIVGRPR HQGVMVGMGQ
 51 KDSYVGDEAQ SKRGILTLKY PIEHGIVTNW DDMEKIWHHT FYNELRVAPE
101 EHPVLLTEAP LNPKANREKM TQIMFETFNT PAMYVAIQAV LSLYASGRTT
151 GIVLDSGDGV SHTVPIYEGY ALPHAILRLD LAGRDLTDYL MKILTERGYT
201 FTTTAEREIV RDIKEKLCYV ALDFEQEMTT AASSSSLEKS YELPDGQVIT
251 IGNERFRCPE ALFQPSFLGM ESCGIHETTY NSIMKCDVDI RKDLYANTVL
301 SGGTTMYPGI ADRMQKEITA LAPSTMKIKI IAPPERKYSV WIGGSILASL
351 STFQQMWISK QEYDESGPSI VHRKCF
```

B

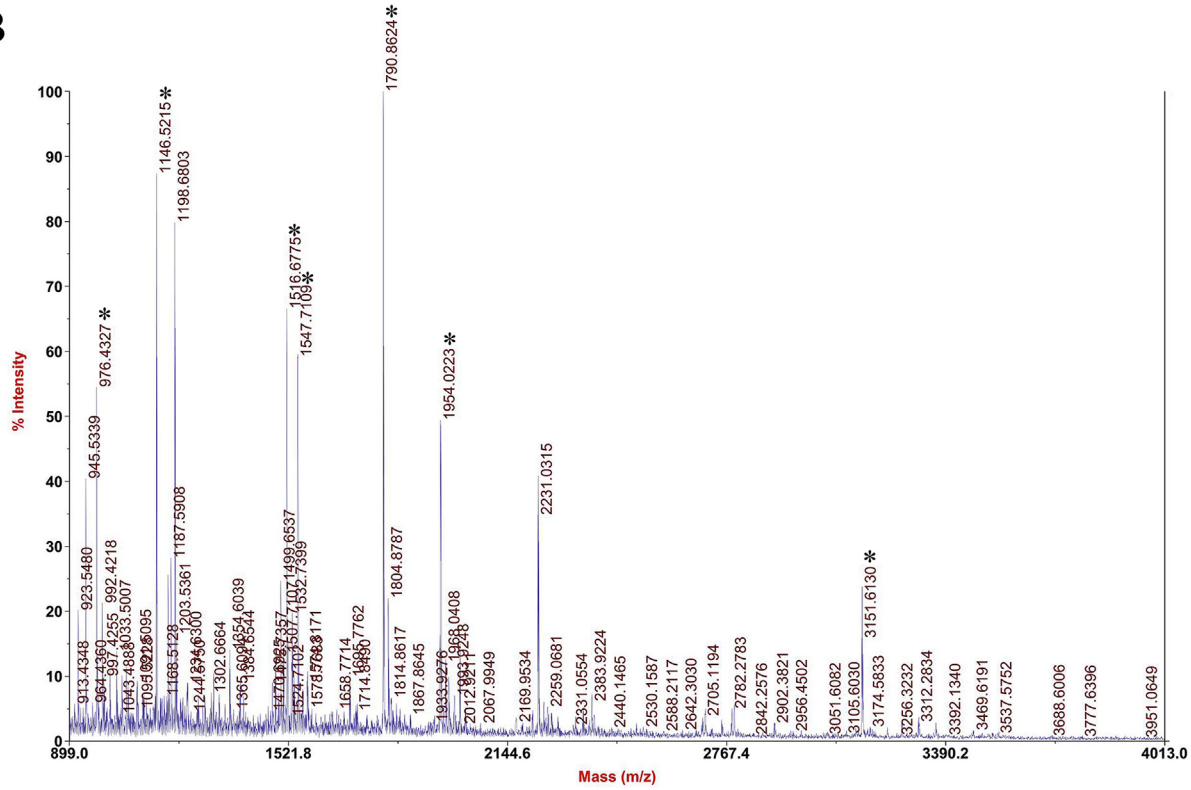

Fig. 3. Identification of the protein pulled down with GTP-bound GST-Rab7 by mass spectrometric analysis. Peptides were produced by tryptic digestion. A, the tryptic peptides that match to β-actin sequence of *L. vannamei* were shown in red; B, the matched peaks were marked by asterisks. (For interpretation of the references to color in this figure legend, the reader is referred to the Web version of this article.)

3.4. Confirmation of the Rab7 binding to β-actin by GST pull-down and ELISA

SDS-PAGE and western blotting revealed that GST-Rab7 could efficiently pull down His-β-actin and β-actin in hemocyte lysate, indicating that Rab7 interacted with β-actin both *in vitro* (Fig. 5, lane 9) and *in vivo* (Fig. 5, lane 10).

Increasing His-Rab7 concentration in ELISAs enhanced its ability to bind to His-β-actin and the hemocyte lysate, whereas for control protein, OD value was approximately constant when His-Rab7 concentrations increased (Fig. 4). Therefore, His-Rab7 binding to both His-β-actin and hemocyte lysate was specific and dose-dependent.

3.5. Cross-interaction between β-actin, VP28 and Rab7

We set out to study the interaction between the three proteins by a series of pull-down experiments. To study whether the interaction between VP28 and Rab7 as well as β-actin is direct, we used purified GST-VP28 to pull down purified His-Rab7 and His-β-actin respectively. These experiments revealed that, GST-VP28 efficiently pulled down His-Rab7 (Fig. 5, lane 12), no interaction was detected between GST-VP28 and His-β-actin (Fig. 5, lane 11).

Using purified proteins, whether Rab7 is able to bridge VP28 and β-actin and thereby form a tripartite complex was next tested. As expected, GST-VP28 pulled down both His-Rab7 and His-β-actin (Fig. 5, lane 13). This indicated that Rab7 is required to bridge VP28 and β-actin.

3.6. Co-localization of β-actin and Rab7 in the hemocytes of shrimp infected with WSSV

To co-localize β-actin and Rab7 in hemocytes, rabbit anti-β-actin-PAbs and mouse anti-Rab7 Mab were used for probing β-actin (red) and Rab7 (green) respectively. At 12 h post WSSV infection, it was observed that some of the green fluorescence was co-localized with red fluorescence (Fig. 6).

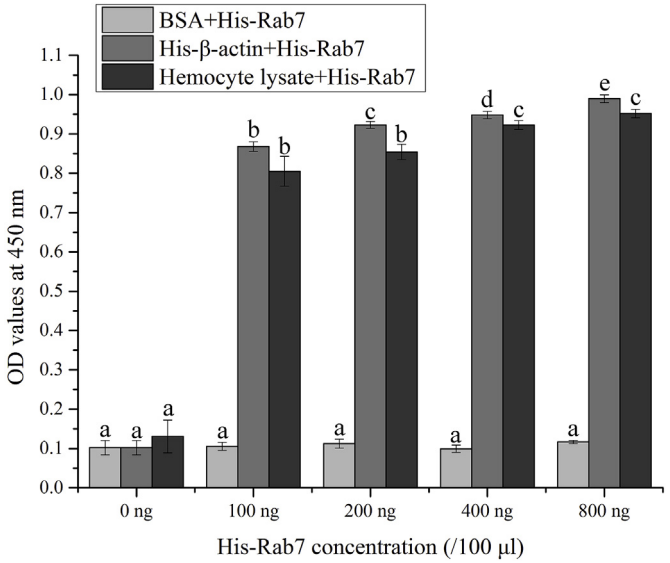

Fig. 4. ELISA assays demonstrated that Rab7 binding to β-actin was specific. His-β-actin (2 μg/well), BSA (2 μg/well) and hemocyte lysate (10 μg/well) were coated to a 96-well plate and incubated with various amounts of purified His-Rab7 (0 ng, 100 ng, 200 ng, 400 ng, 800 ng). Each column and vertical bar represents the mean ± SD of triplicate determinations. The different letters above the column indicate significant differences ($p < 0.05$) among the OD_{450} values at different His-Rab7 concentrations for each coated protein.

3.7. Co-localization of WSSV and β-actin, Rab7 in the hemocytes of shrimp infected with WSSV

For double immuno-labeling, mouse anti-WSSV Mab and mouse anti-Rab7 Mab originating in the same species were successfully labled with green fluorescence (Fig. 7, B) and red fluorescence (Fig. 7, C) respectively. At 12 h post WSSV infection, it was observed that most of the green fluorescence was co-localized with red fluorescence. Especially, the hemocytes presented two areas where both green and red strong fluorescence were densely distributed and co-localized (indicated by the asterisks in Fig. 8). However, there was little sign that green and red fluorescence were co-localized at 12 h post WSSV infection, which were used for labeling anti-WSSV Mab and anti-β-actin-Pabs respectively (Fig. 7, H).

3.8. Neutralization of WSSV activity by recombinant proteins in vivo

For *in vivo* neutralization experiments using shrimp, with the exception of the PBS injection group, mortalities in the other three groups of shrimp increased steadily after WSSV challenge (Fig. 8). Furthermore, 100% mortality occurred within 9 d in the positive control group (shrimp challenged with WSSV only). The cumulative motilities were higher than in the positive control group within 6 d for shrimp injected with the inoculum containing WSSV mixed with His-β-actin, indicating that His-β-actin facilitated the infection of WSSV. While, the cumulative motilities were lower than WSSV plus His-β-actin injected group when equal mol His-β-actin and His-Rab7 were added to WSSV inoculums. Furthermore, the lowest cumulative mortalities occurred in WSSV plus His-Rab7 group except that no shrimp mortality occurred in the PBS injected group (negative control group). Therefore, recombinant His-β-actin accelerated the infection of WSSV, conversely, recombinant His-Rab7 delayed WSSV infection in shrimp.

4. Discussion

As a WSSV binding protein, Rab7 has been identified to be involved in WSSV infection and this molecule could recruit cytoplasmic dynein, dynactin, RILP and ORP1L to form a complex to regulate MT minus-directed transport of endosomes [20]. In the present work, we planned to characterize the proteins that had been identified as Rab7 effectors such as RILP, ORP1L, which participated together in the transport of WSSV endosome. By accident, the protein pulled down with GST-Rab7 was microfilament actin not MT-associated proteins. During WSSV infection, β-actin has been characterized to play vital roles through

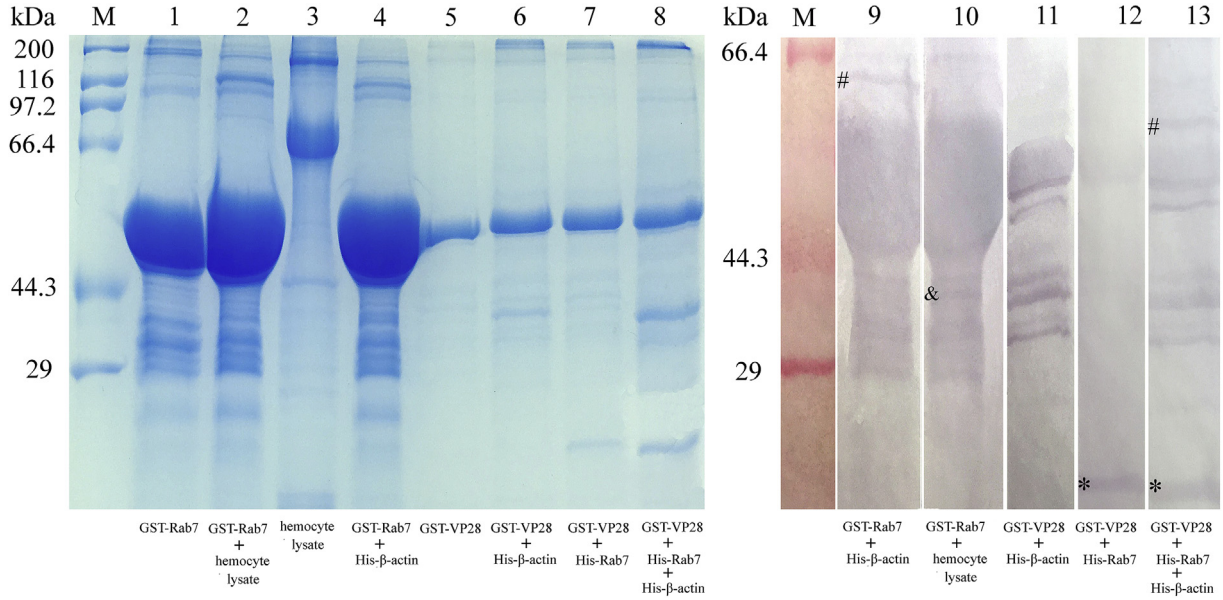

Fig. 5. SDS-PAGE and western blotting cinfirmed the cross-interaction between β-actin, VP28 and Rab7. All the lanes in western blotting were incubated with both rabbit anti-β-actin Pabs and mouse anti-Rab7 Mab. The positive bands indicating His-β-actin, His-Rab7 and β-actin in hemocyte lysate are shown as (#), (*) and (&) respectively. Lane M, Molecular mass marker; lane 1, protein profile of glutathione beads coupled with purified GST-Rab7; lane 2, the profile of retained proteins with GST-Rab7 from hemocyte lysate; lane 3, protein profile of hemocyte lysate; lane 4, the profile of retained proteins with purified GST-Rab7 and His-β-actin; lane 5, protein profile of glutathione beads coupled with purified GST-VP28; lane 6, 7, 8, the profile of retained proteins with purified GST-VP28 and His-β-actin, His-Rab7 as well as the mixture of His-β-actin and His-Rab7 respectively; lane 9, 10, 11, 12, 13, mouse anti-Rab7 Mab and rabbit anti-β-actin-PAbs recognized the corresponding protein of lane 4, 2, 6, 7, 8 in SDS-PAGE.

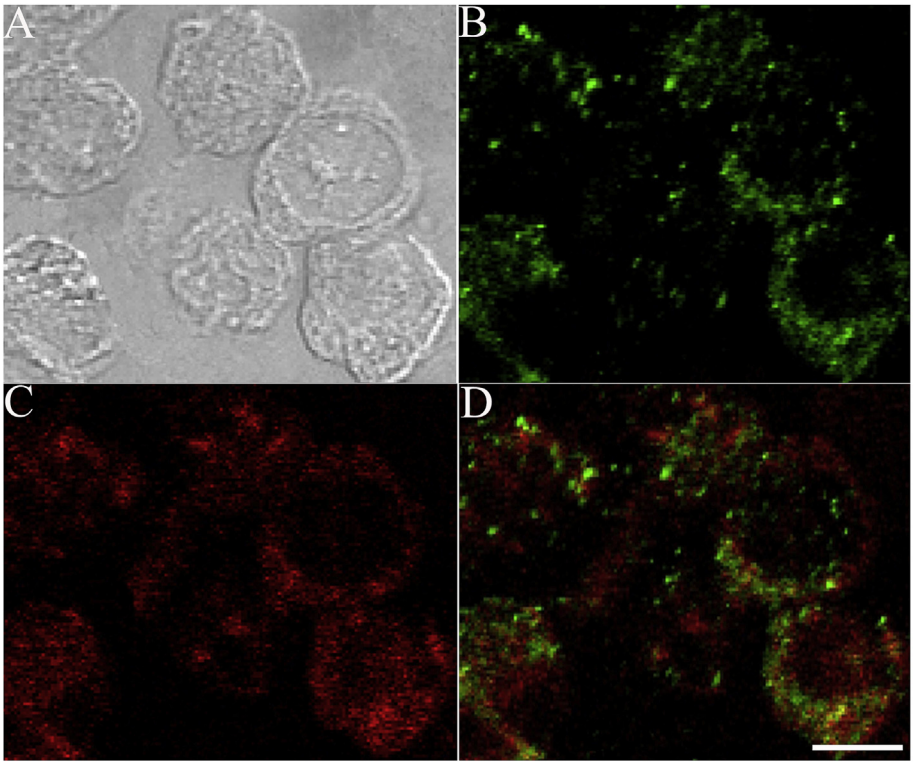

Fig. 6. Co-localization of β-actin and Rab7 in hemocytes of the virus-infected shrimp. A, hemocytes in the bright field; B, localization of Rab7 using FITC (green) in shrimp hemocytes; C, localization of β-actin using Cy3 (red) in shrimp hemocytes; D, the merged imagine showing the localization of both Rab7 and β-actin. Bar = 10 μm. (For interpretation of the references to color in this figure legend, the reader is referred to the Web version of this article.)

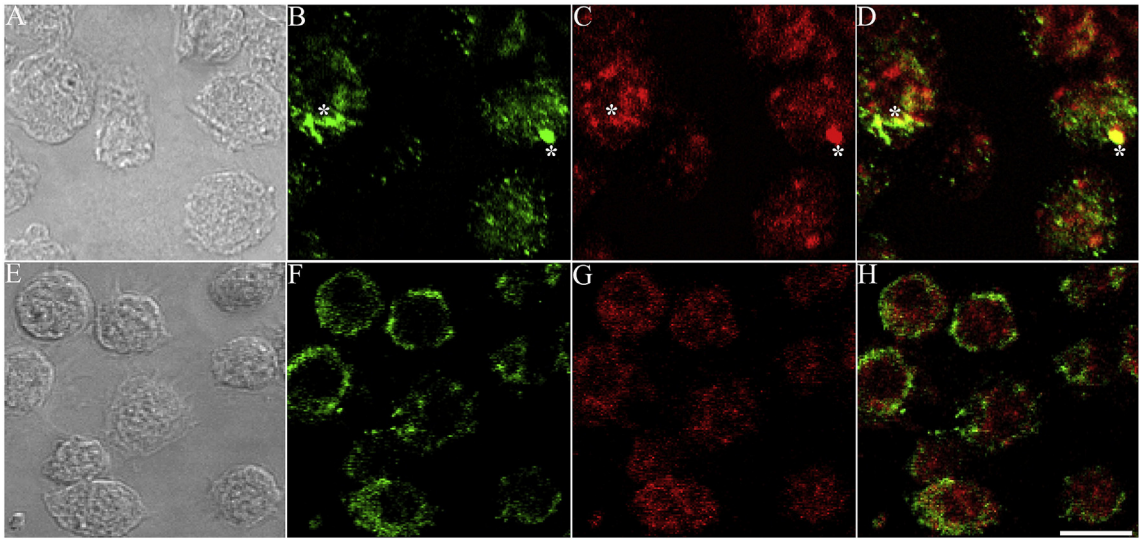

Fig. 7. Co-localization of WSSV and β-actin, Rab7 in hemocytes of the virus-infected shrimp. A and E, hemocytes in the bright field; B and F, localization of WSSV and using FITC (green) in shrimp hemocytes; C, localization of Rab7 using Cy3 (red) in shrimp hemocytes; G, localization of β-actin using Cy3 (red) in shrimp hemocytes; D, the merged imagine showing the co-localization of WSSV and Rab7 in hemocytes; H, the merged imagine showing the co-localization of WSSV and β-actin in hemocytes. Two areas where both green and red strong fluorescence were densely distributed and co-localized were indicated by the asterisks. Bar = 10 μm. (For interpretation of the references to color in this figure legend, the reader is referred to the Web version of this article.)

interacting with WSSV structural protein VP26 [21,22].

Actin functions in a wide range of attachment and entry processes that are critical to the very earliest infection stages of viruses which use the actin cytoskeleton to control entry and short-range transport at the cell periphery [23]. Viruses including the large DNA virus exploit actin-mediated endocytic pathways to infect a wide range of cell types [24–26]. Combined with the specific interaction of β-actin with WSSV VP26 documented previously, the results that recombinant His-β-actin significantly enhanced the infection of WSSV to the shrimp might be due to the essential role of β-actin in the endocytic pathway of WSSV, which had been verified to enter into the host cell through caveolin and clathrin-mediated endocytosis [8–10,21,22]. Meanwhile, β-actin was co-localized with WSSV in hemocyte in the present work which further revealed the close relation between β-actin and endosome trafficking during WSSV infection.

Most viruses switch from the actin cytoskeleton to MT tracks to promote long-range movement to the replication region [27,28]. It has been well documented that multiple host factors such as focal adhesion proteins and ezrin-radixin-moesin (ERM) family members could regulate actin-MT cross-linking and influence infection of viruses [29–31]. In shrimp, a focal adhesion proteins, focal adhesion kinase, was also characterized to involve in WSSV infection and host defense [32,33].

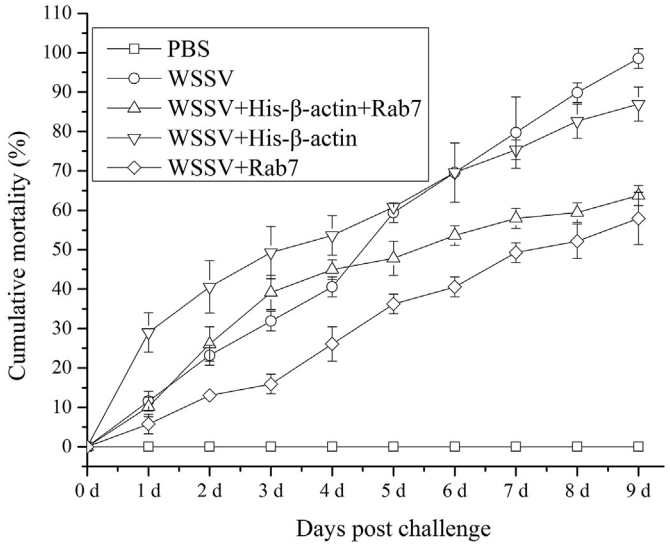

Fig. 8. Cumulative post-challenge shrimp mortality. Shrimp were challenged with inoculum containing WSSV mixed with His-β-actin (WSSV + His-β-actin), or inoculum containing WSSV mixed with His-Rab7 (WSSV + His-Rab7), or inoculum containing WSSV mixed with both His-β-actin and His-Rab7 (WSSV + His-β-actin + His-Rab7). Shrimp injected with inoculum containing WSSV, or injected with PBS only, were positive and negative controls respectively. Each symbol and vertical bars represented the mean ± SD (n = 3).

However, the mechanism that mediates WSSV endosome switching from the actin cytoskeleton to MT and the very host proteins involve in this biological process are still not clear. During WSSV infection, the essential role of Rab7 was reflected in its specific binding with VP28 and both Rab7 gene sequence-specific dsRNA and the recombinant Rab7 all exhibited the ability to delay mortality upon WSSV challenge which were reinforced in this research [4–6]. According to the model for the WSSV life cycle and morphogenesis, Rab7 mediated the travel of WSSV through endosomes [34,35]. These indicated that the delay of WSSV infection by the recombinant Rab7 might be due to the hindrance of WSSV interacting with nature Rab7 in hemocytes, which then interfered the transport of WSSV. Furthermore, the process of endosome trafficking mediated by Rab7 occurred after the endocytosis of WSSV. So, it could be hypothesized that Rab7 participated in the translocation of WSSV endosome from actin cytoskeleton to MT based on its specific interacting and co-localization with β-actin in WSSV infected hemocytes. These results may open the way for the investigation of complex events in early infection of WSSV to the host cells.

Accordingly, Rab7 is involved in governing multiple trafficking processes including the biogenesis of the lysosome, phagosome, autophagosome, and other lysosome-related organelle [36]. This role of Rab7 has been confirmed to be carried out by recruiting cytoplasmic dynein motor to form a complex to regulate MT minus-directed transport of endosomes [36,37]. Dynactin as an essential component of the cytoplasmic dynein motor possesses an actin-like filament whose major component is the actin-related protein Arp1 mediating cargo interactions [38,39]. This actin-related protein Arp1 shares the same number of amino acids and high sequence similarity (97%) and identity (53%) with β-actin in *L. vannamei*. So, there is the possibility that the β-actin characterized in this work is actin-related protein Arp1 as one of the subunits in dynactin. However, little information about Arp1 in shrimp has been documented so far. To decipher the role of β-actin and Rab7 in WSSV translocation, much more works on the relationship between cytoskeletal networks and WSSV need to be done in future.

Acknowledgements

This work was supported by Shandong Provincial Natural Science Foundation, China (ZR2015CL048), Shandong Province Agricultural Innovation Team (SDAIT-12-03) and Hainan Provincial Hey Research and Development Program (ZDYF2018028).

References

[1] J.S. Bonifacino, J. Neefjes, Moving and positioning the endolysosomal system, Curr. Opin. Cell Biol. 47 (2017) 1–8.
[2] J. Huotari, A. Helenius, Endosome maturation, EMBO J. 30 (2011) 3481–3500.
[3] T. Wang, Z. Ming, W. Xiaochun, W. Hong, Rab7: role of its protein interaction cascades in endo-lysosomal traffic, Cell. Signal. 23 (2011) 516–521.
[4] K. Sritunyalucksana, W. Wannapapho, C.F. Lo, T.W. Flegel, PmRab7 is a VP28-binding protein involved in white spot syndrome virus infection in shrimp, J. Virol. 80 (2006) 10734–10742.
[5] J. Xu, F. Han, X. Zhang, Silencing shrimp white spot syndrome virus (WSSV) genes by siRNA, Antivir. Res. 73 (2007) 126e31.
[6] R. Sudhakaran, T. Mekata, T. Kono, M. Inada, S. Okugawa, M. Yoshimine, T. Yoshida, M. Sakai, T. Itami, Double-stranded RNA-mediated silencing of the white spot syndrome virus VP28 gene in kuruma shrimp, *Marsupenaeus japonicus*, Aquacult. Res. 42 (2011) 1153e62.
[7] C.H. Mejía-Ruíz, S. Vega-Peña, P. Alvarez-Ruiz, Escobedo-Bonilla CM. Double-stranded RNA against White Spot Syndrome Virus (WSSV) vp28 or vp26 reduced susceptibility of *Litopenaeus vannamei* to WSSV, and survivors exhibited decreased susceptibility in subsequent re-infections, J. Invertebr. Pathol. 107 (2011) 65e8.
[8] Z.J. Huang, S.T. Kang, J.H. Leu, L.L. Chen, Endocytic pathway is indicated for white spot syndrome virus (WSSV) entry in shrimp, Fish Shellfish Immunol. 35 (2013) 707–715.
[9] H. Duan, S. Jin, Y. Zhang, F. Li, J. Xiang, Granulocytes of the red claw crayfish *Cherax quadricarinatus* can endocytose beads, *E. coli* and wssv, but in different ways, Dev. Comp. Immunol. 46 (2014) 186–193.
[10] J. Huang, F. Li, J. Wu, F. Yang, White spot syndrome virus enters crayfish hematopoietic tissue cells via Clathrin-mediated endocytosis, Virology 486 (2015) 35–43.
[11] I. Jordens, M. Fernandez-Borja, M. Marsman, S. Dusseljee, L. Janssen, J. Calafat, H. Janssen, R. Wubbolts, J. Neefjes, The Rab7 effector protein RILP controls lysosomal transport by inducing the recruitment of dynein-dynactin motors, Curr. Biol. 11 (2001) 1680–1685.
[12] M. Johansson, N. Rocha, W. Zwart, I. Jordens, L. Janssen, C. Kuijl, V.M. Olkkonen, J. Neefjes, Activation of endosomal dynein motors by stepwise assembly of Rab7-RILP-p150^{Glued}, ORP1L, and the receptor betalll spectrin, J. Cell Biol. 176 (2007) 459–471.
[13] F. Guerra, C. Bucci, Multiple roles of the small GTPase Rab7, Cells 5 (2016) 34.
[14] M. Wu, T. Wang, E. Loh, W. Hong, H. Song, Structural basis for recruitment of RILP by small GTPase Rab7, EMBO J. 24 (2005) 1491–1501.
[15] T.K. Sato, P. Rehling, M.R. Peterson, S.D. Emr, Class C Vps protein complex regulates vacuolar SNARE pairing and is required for vesicle docking/fusion, Mol. Cell. 6 (2000) 661–671.
[16] D.F. Seals, G. Eitzen, N. Margolis, W.T. Wickner, A. Price, A Ypt/Rab effector complex containing the Sec1 homolog Vps33p is required for homotypic vacuole fusion, Proc. Natl. Acad. Sci. U.S.A. 97 (2000) 9402–9407.
[17] C.F. Lo, J.H. Leu, C.H. Ho, C.H. Chen, S.E. Peng, Y.T. Chen, C.M. Chou, P.Y. Yeh, C.J. Huang, H.Y. Chou, C.H. Wang, G.H. Kou, Detection of baculovirus associated with white spot syndrome (WSBV) in penaeid shrimps using polymerase chain reaction, Dis. Aquat. Org. 25 (1996) 133–141.
[18] W. Zhan, X. Wang, J. Chen, J. Xing, H. Fukuda, Elimination of shrimp endogenous alkaline phosphatase background and development of enzyme immunoassays for the detection of white spot syndrome virus (WSSV), Aquaculture 239 (2004) 15–21.
[19] W. Yingvilasprasert, P. Supungul, A. Tassanakajon, *Pm*TBC1D20, a Rab GTPase-activating protein from the black tiger shrimp, *Penaeus monodon*, is involved in white spot syndrome virus infection, Dev. Comp. Immunol. 42 (2014) 302–310.
[20] J.M. Hyttinen, M. Niittykoski, A. Salminen, K. Kaarniranta, Maturation of autophagosomes and endosomes: a key role for Rab7, Biochim. Biophys. Acta 1833 (2013) 503–510.
[21] X. Xie, F. Yang, Interaction of white spot syndrome virus VP26 protein with actin, Virology 336 (2005) 93–99.
[22] B.L. Liu, X.Q. Tang, W.B. Zhan, Interaction between white spot syndrome virus VP26 and hemocyte membrane of shrimp, *Fenneropenaeus chinensis*, Aquaculture 314 (2011) 13–17.
[23] D. Walsh, M.H. Naghavi, Exploitation of cytoskeletal networks during early viral infection, Trends Microbiol. 27 (2019) 39–50.
[24] B. Hernaez, C. Alonso, Dynamin- and clathrin-dependent endocytosis in african swine fever virus entry, J. Virol. 84 (2010) 2100–2109.
[25] K.C. Huang, Z. Yasruel, C. Guérin, P.C. Holland, J. Nalbantoglu, Interaction of the Coxsackie and adenovirus receptor (CAR) with the cytoskeleton: binding to actin, FEBS Lett. 581 (2007) 2702–2708.
[26] Y. Baktash, A. Madhav, K.E. Coller, G. Randall, Single particle imaging of polarized hepatoma organoids upon hepatitis C virus infection reveals an ordered and sequential entry process, Cell Host Microbe 23 (2018) 382–394.
[27] M.P. Dodding, M. Way, Coupling viruses to dynein and kinesin-1, EMBO J. 30 (2011) 3527–3539.
[28] M.H. Naghavi, D. Walsh, Microtubule regulation and function during virus infection, J. Virol. 91 (2017) e00538-17.
[29] M.H. Naghavi, S. Valente, T. Hatziioannou, K. de Los Santos, Y. Wen, C. Mott, G.G. Gundersen, S.P. Goff, Moesin regulates stable microtubule formation and limits retroviral infection in cultured cells, EMBO J. 26 (2007) 41–52.

[30] J. Haedicke, K. de Los Santos, S.P. Goff, M.H. Naghavi, The Ezrin-radixin-moesin family member ezrin regulates stable microtubule formation and retroviral infection, J. Virol. 82 (2008) 4665–4670.
[31] C. Brown, S.G. Morham, D. Walsh, M.H. Naghavi, Focal adhesion proteins talin-1 and vinculin negatively affect paxillin phosphorylation and limit retroviral infection, J. Mol. Biol. 410 (2011) 761–777.
[32] M. Zhang, H. Wang, D. Li, X. Xu, A novel focal adhesion kinase from *Marsupenaeus japonicus* and its response to WSSV infection, Dev. Comp. Immunol. 33 (2009) 533–539.
[33] H. Lu, L. Ruan, X. Xu, An immediate-early protein of white spot syndrome virus modulates the phosphorylation of focal adhesion kinase of shrimp, Virology 419 (2011) 84–89.
[34] C.M. Escobedo-Bonilla, V. Alday-Sanz, M. Wille, P. Sorgeloos, M.B. Pensaert, H.J. Nauwynck, A review on the morphology, molecular characterization, morphogenesis and pathogenesis of white spot syndrome virus, J. Fish. Dis. 31 (2008) 1–18.
[35] B. Verbruggen, L. Bickley, R. van Aerle, K. Bateman, G. Stentiford, E. Santos, C. Tyler, Molecular mechanisms of white spot syndrome virus infection and perspectives on treatments, Viruses 8 (2016) 23.
[36] S.L. Reck-Peterson, W.B. Redwine, R.D. Vale, A.P. Carter, The cytoplasmic dynein transport machinery and its many cargoes, Nat. Rev. Mol. Cell Biol. 19 (2018) 382–398.
[37] G. Cantalupo, P. Alifano, V. Roberti, C.B. Bruni, C. Bucci, Rab-interacting lysosomal protein (RILP): the Rab7 effector required for transport to lysosomes, EMBO J. 20 (2001) 683–693.
[38] L. Urnavicius, K. Zhang, A.G. Diamant, C. Motz, M.A. Schlager, M. Yu, N.A. Patel, C.V. Robinson, A.P. Carter, The structure of the dynactin complex and its interaction with dynein, Science 347 (2015) 1441–1446.
[39] H. Imai, A. Narita, Y. Maéda, T.A. Schroer, Dynactin 3D structure: implications for assembly and dynein binding, J. Mol. Biol. 426 (2014) 3262–3271.